Effect of Protein Microenvironment on Tyrosyl Radicals. A High-Field (285 GHz) EPR, Resonance Raman, and Hybrid Density Functional Study

Anabella Ivancich,*,‡ Tony A. Mattioli,†,§ and Sun Un‡

Contribution from the Section de Bioénergétique and Section de Biophysique des Protéines et des Membranes, URA 2096 CNRS, Département de Biologie Cellulaire et Moléculaire, CEA Saclay, 91191 Gif-sur-Yvette, France

Received February 22, 1999. Revised Manuscript Received April 28, 1999

Abstract: The protein environment appears to regulate the biological function of tyrosyl radicals (Tommos, C.; Babcock, G. T. *Acc. Chem. Res.* **1998**, *31*, 18−25). Vibrational spectroscopy and electron paramagnetic resonance (EPR) techniques have been used to characterize tyrosyl radicals. In this work, we have investigated the relationship between the *g* values and the vibrational spectra of tyrosyl radicals (Tyr•) in different protein microenvironments by combining experimentally determined values and molecular orbital calculations. High-field (285 GHz) electron paramagnetic resonance (HF-EPR) and resonance Raman spectroscopies were applied to obtain the *g* values and the vibrational frequencies, respectively, of the tyrosyl radical ($Tyr^{\bullet}_{CAT}$) previously reported as a heme catalase intermediate [(Fe(IV)═O) Tyr•] (Ivancich, A.; Jouve, H. M.; Gaillard, J. *J. Am. Chem. Soc.* **1996**, *118*, 12852−12853. Ivancich, A., Jouve, H. M.; Sartor, B.; Gaillard, J. *Biochemistry* **1997**, *36*, 9356−9364). The effect of the protein microenvironment on the catalase tyrosyl radical was examined by varying the pH between 6.7 and 4.5. The broadness of the g_x edge in the $Tyr^{\bullet}_{CAT}$ HF-EPR spectrum was interpreted as arising from a distribution in hydrogen bond strengths. The observed g_x values of 2.0073(8) at pH 6.7 and 2.0076(2) at pH 4.5 indicated the presence of one or two hydrogen bonds to the $Tyr^{\bullet}_{CAT}$. The asymmetric shape of the g_x edge of the $Tyr^{\bullet}_{CAT}$ spectrum was attributed to the presence of a minor feature centered at 2.0065(5) for pH 6.7 and at 2.0082(4) for pH 4.5. These g_x values are comparable to those reported for the hydrogen-bonded γ-generated tyrosyl radical in Tyr-HCl crystals (2.00670: Fasanella, E. L.; Gordy, W. *Proc. Natl. Acad. Sci. U.S.A.* **1969**, *62*, 299−304) and the non-hydrogen-bonded Tyr• in *Escherichia coli* ribonucleotide reductase (RNR) (2.00866: Un, S.; Atta, M.; Fontecave, M.; Rutherford, A. W. *J. Am. Chem. Soc.* **1995**, *117*, 10713−10719). One- and two-water complexes of *p*-methylphenoxy and phenoxy radicals were used to model the protein tyrosyl radical. Semiempirical MNDO molecular orbital calculations were used to analyze the effect of hydrogen bonds on the *g* values of the *p*-methylphenoxy radical. *Ab initio* density functional calculations were carried out to investigate the effect of hydrogen bond strengths on the vibrational frequencies of the radical, in particular the ν_{7a}(C−O) stretching mode. The calculated *g* values and vibrational frequencies were in very good agreement with the experimentally observed values for the tyrosyl radicals in catalase, *E. coli* RNR, and photosystem II. In contrast to the g_x values (*g*-tensor component in the C−O direction of the radical), the density functional calculations predict a nonmonotonic behavior of the vibrational frequency of the ν_{7a}(C−O) stretching mode as a function of hydrogen bond distance. Specifically, for hydrogen bond distances shorter than 1.7 Å, a sharp decrease of the ν_{7a} vibrational frequencies was observed. In contrast, for hydrogen bond distances longer than 1.7 Å, an increase of the vibrational frequencies was observed, as compared to the non-hydrogen-bonded situation.

Introduction

An increasing number of amino acid radicals involved in the redox chemistry of metalloproteins have been identified in recent years.[1] In particular, tyrosyl radicals (Tyr•) have been proposed to have a specific functional role in electron- and/or proton-transfer processes in several proteins.[2−4] Recently, a tyrosyl radical has been reported as a heme catalase intermediate [(Fe(IV)═O) Tyr•].[5,6] All these tyrosyl radicals have been identified by using magnetic resonance techniques combined, in some cases, with deuterium labeling and site-directed mutagenesis of the tyrosine residues. Information concerning the electronic structure of the radicals and their interaction with the protein has been obtained using electron paramagnetic resonance (EPR) techniques. The spin density distribution of Tyr• has been

* Corresponding author. E-mail: ivancich@dsvidf.cea.fr.
‡ Section de Bioénergétique.
† Section de Biophysique des Protéines et des Membranes.
§ Present address: IDS, Intelligent Detection Systems, 152 Cleopatra Dr., Nepean, Ontario K2G5X2, Canada. E-mail: tmattioli@idsdetection.com

(1) (a) Sigel, H., Sigel, A., Eds. *Metalloenzymes Involving Amino Acid-Residue and Related Radicals Metal Ions in Biological Systems*; Marcell Dekker: New York, 1994; Vol. 30. (b) Stubbe, J.; van der Donk, W. A. *Chem. Rev.* **1998**, *98*, 705−762.
(2) Tommos, C.; Babcock, G. T. *Acc. Chem. Res.* **1998**, *31*, 18−25.
(3) Gräslund, A.; Sahlin, M. *Annu. Rev. Biophys. Biomol. Struct.* **1996**, *25*, 259−286.
(4) Siegbahn, P. E. M.; Eriksson, L.: Himo, F.; Pavlov, M. *J. Phys. Chem. B* **1998**, *102*, 10622−10629.
(5) Ivancich, A.; Jouve, H. M.; Gaillard, J. *J. Am. Chem. Soc.* **1996**, *118*, 12852−12853.
(6) Ivancich, A.; Jouve, H. M.; Sartor, B.; Gaillard, J. *Biochemistry* **1997**, *36*, 9356−9364.

10.1021/ja990562m CCC: $18.00
Published on Web 06/06/1999

determined from the proton hyperfine couplings measured by ENDOR and ESEEM spectroscopies.[7−11] ENDOR spectroscopy and high-field EPR have been used to assess the hydrogen bond state of tyrosyl radicals.[5,6,10−14]

The protein is expected to exert a considerable influence on the physicochemical properties of tyrosyl radicals. Vibrational spectroscopy is a standard technique used for monitoring structural changes of chromophores induced by the protein environment. The tyrosyl radicals from *Escherichia coli* ribonucleotide reductase (RNR),[15] galactose, and glyoxal oxidases[16,17] have been characterized by resonance Raman (RR) techniques using excitation wavelengths resonant with the radical electronic absorption band, which specifically enhanced the vibrational stretching modes of the radicals.[18] The tyrosyl radicals in photosystem II (PSII) have been investigated by using Fourier transform infrared spectroscopy (FTIR), a differential vibrational technique which takes advantage of the light-induced radical formation.[19−22] The vibrational frequency of the band assigned to the C−O stretching mode (ν_{7a}) of the tyrosyl radical reflects the presence or absence, as well as the strength, of the hydrogen bond(s) to the radical. The ν_{7a} mode is sensitive to the local electronic environment and is influenced by hydrogen bonds and metal coordination of the tyrosyl radical.[23] Recently, it has been shown that *g* values can also be used to probe the local protein environment of radicals, specifically electrostatic and hydrogen-bonding effects.[13,24,25] The required accurate values of the *g*-tensor and the *g*-anisotropy were measured by using HF-EPR on the tyrosyl radicals of PSII,[13,26,27] RNR,[13,28−32] and catalase.[5] It has been shown that, like the vibrational frequency of the ν_{7a} mode, the *g*-tensor component in the direction of the C−O bond (g_x) of these tyrosyl radicals is also sensitive to local electrostatic effects. Consequently, the g_x value is indicative of the presence and the strength of hydrogen bond interactions to the tyrosyl radicals. However, the relationship between the ν_{7a} vibrational frequency and the g_x value has not been established.

The 1498-cm^{-1} band observed in the RR spectrum of *E. coli* RNR, excited at 406.7 nm, has been assigned to the vibrational frequency of the C−O stretching mode (ν_{7a}) of the tyrosyl radical.[15] The absence of frequency shifts in the RR spectrum after deuterium exchange of the buffer solution was attributed to the lack of proton association to the RNR tyrosyl radical ($Tyr^{\bullet}_{RNR}$).[15] The crystal structure of the *E. coli* RNR confirmed that the radical is in a hydrophobic environment and not engaged in hydrogen bond interactions.[33,34] The g_x value obtained from the HF-EPR measurements on the *E. coli* $Tyr^{\bullet}_{RNR}$ was 2.0086(6) (or 2.0091(2), see Table 1), a value which is significantly higher than that of the hydrogen-bonded $Tyr^{\bullet}$ in the γ-irradiated Tyr-HCl crystals.[35] Semiempirical calculations confirmed that such a high g_x value is consistent with the absence of a hydrogen bond.[13] The bands observed at 1503 and 1512/3 cm^{-1} in the FTIR difference spectrum of wild-type and a mutant *Synechocystis* PSII were assigned to the C−O stretching modes (ν_{7a}) of $Tyr^{\bullet}_{D}$ and $Tyr^{\bullet}_{Z}$, respectively.[21,22] Comparison of such vibrational frequencies with those observed in the FTIR difference spectra of *in vitro* tyrosyl radicals, together with isotopic replacement on the PSII tyrosyl radicals, leads to the conclusion that both $Tyr^{\bullet}_{D}$ and $Tyr^{\bullet}_{Z}$ are hydrogen bonded but with different hydrogen bond strengths.[22] The HF-EPR spectrum of the same *Synechocystis* PSII tyrosyl radicals showed that both $Tyr^{\bullet}_{D}$ and $Tyr^{\bullet}_{Z}$ have identical nominal *g* values, with a g_x of 2.0074(0), an intermediate value between those observed for the tyrosyl radicals in *E. coli* RNR and those in the Tyr-HCl (see Table 1). This result was attributed to the presence of at least one hydrogen bond to each tyrosyl radical.[13,27] The difference between the two PSII radicals was the observed broadness of the g_x edge of $Tyr^{\bullet}_{Z}$ HF-EPR spectrum as compared to that of $Tyr^{\bullet}_{D}$. This was interpreted as arising from a distribution in hydrogen bond strengths in $Tyr^{\bullet}_{Z}$, in contrast to a well-ordered hydrogen bonding in $Tyr^{\bullet}_{D}$.[27] Even though the interpretations of the HF-EPR and FTIR results are in qualitative agreement concerning the presence of a hydrogen bond for both PSII tyrosyl radicals, they appear to differ in the estimation of hydrogen bond strengths. Hence, the existing experimental data do not present a clear picture of the correlation between HF-EPR and vibrational spectroscopy results.

In this work, we specifically address the relationship between the *g* values and the vibrational spectra of tyrosyl radicals$^{\bullet}$. The effect of the protein microenvironment on the *g*-tensor component in the direction of the C−O bond (g_x value) of the

(7) Hoganson, C. W.; Babcock, G. T. *Biochemistry* **1988**, *27*, 5848−5855.
(8) Bender, C. J.; Sahlin, M.; Babcock, G. T.; Barry, B. A.; Chandrashekar, T. K.; Salowe, S. P.; Stubbe, J.; Lindström, B.; Petersson, L.; Ehrenberg, A.; Sjöberg, B.-M. *J. Am. Chem. Soc.* **1989**, *111*, 8076−8083.
(9) Rigby, S. E. J.; Nugent, J. H.; O'Malley, P. J. *Biochemistry* **1994**, *33*, 1734−1742.
(10) Warncke, K.; Babcock, G. T.; McCracken, J. *J. Am. Chem. Soc.* **1994**, *116*, 7332−7340.
(11) Tommos, C.; Tang, X.-S.; Warncke, K.; Hoganson, C. W.; Styring, S.; McCracken, J.; Diner, B. A.; Babcock, G. T. *J. Am. Chem. Soc.* **1995**, *117*, 10325−10335.
(12) Tang, X.-S.; Chisholm, D. A.; Dismukes, C. G.; Brudvig, G. W.; Diner, B. A. *Biochemistry* **1993**, *32*, 13742−13748.
(13) Un, S.; Atta, M.; Fontecave, M.; Rutherford, A. W. *J. Am. Chem. Soc.* **1995**, *117*, 10713−10719.
(14) Campbell, K. A.; Peloquin, J. M.; Diner, B. A.; Tang, X.-S.; Chisholm, D. A.; Britt, R. D. *J. Am. Chem. Soc.* **1997**, *119*, 4787−4788.
(15) Backes, G.; Sahlin, M.; Sjoberg, B. M.; Loehr, T. M.; Sanders-Loehr, J. *Biochemistry* **1989**, *28*, 1923−1929.
(16) Whittaker, M. M.; De Vito, V. L.; Asher, S. A.; Whittaker, J. W. *J. Biol. Chem.* **1989**, *264*, 7104−7106.
(17) Whittaker, M. M.; Kersten, P. J.; Nakamura, N.; Sanders-Loehr, J.; Schweizer, E. S.; Whittaker, J. W. *J. Biol. Chem.* **1996**, *271*, 681−687.
(18) Tripathi, G. N. R.; Schuler, R. H. *J. Chem. Phys.* **1984**, *1*, 5129−5133.
(19) (a) Hienerwadel, R.; Boussac, A.; Breton, J.; Berthomieu, C. *Biochemistry* **1996**, *35*, 15447−15460. (b) Hienerwadel, R.; Boussac, A.; Breton, J.; Diner, B.; Berthomieu, C. *Biochemistry* **1997**, *36*, 14712−14723.
(20) Zhang, H.; Razeghifard, M. R.; Fischer, G.; Wydrzynski, T. *Biochemistry* **1997**, *36*, 11762−11768.
(21) Noguchi, T.; Inoue, Y.; Tang, X.-S. *Biochemistry* **1997**, *36*, 14705−14711.
(22) Berthomieu, C.; Hienerwadel, R.; Boussac, A.; Breton, J.; Diner, B. A. *Biochemistry* **1998**, *37*, 10547−10554.
(23) Schnepf, R.; Sokolowski, A.; Müller, J.; Bachler, V.; Wieghardt, K.; Hildebrandt, P. *J. Am. Chem. Soc.* **1998**, *120*, 2352−2364.
(24) Burghaus, O.; Plato, M.; Rohrer, M.; Möbius, K.; MacMillan, F.; Lubitz, W. *J. Phys. Chem.* **1993**, *97*, 7693−7647.
(25) Knüpling, M.; Törring, J. T.; Un, S. *Chem. Phys.* **19XX**, *219*, 291−304.
(26) Un, S.; Brunel, L.-C.; Brill, T. M.; Zimmerman, J.-L.; Rutherford, A. W. *Proc. Natl. Acad. Sci. U.S.A.* **1994**, *91*, 5262−5266.
(27) Un, S.; Tang, X.-S.; Diner, B. A. *Biochemistry* **1996**, *35*, 679−684.
(28) Gerfen, G. J.; Bellew, B. F.; Un, S.; Bollinger, J. M.; Stubbe, J.; Griffin, R. G.; Singel, D. J. *J. Am. Chem. Soc.* **1993**, *115*, 6420−6421.
(29) Allard, P.; Barra, A.-L.; Andersson, K. K.; Schmidt, P. P.; Atta, M.; Gräslund, A. *J. Am. Chem. Soc.* **1996**, *118*, 895−896.
(30) Schmidt, P. P.; Andersson, K. K.; Barra, A.-L.; Thelander, L.; Gräslund, A. *J. Biol. Chem.* **1996**, *271*, 23615−23618.
(31) van Dam, P. J.; Willems, J. P.; Schmidt, P. P.; Pötsch, S.; Barra, A. L.; Hagen, W. R.; Hoffman, B. M.; Andersson, K. K.; Gräslund, A. *J. Am. Chem. Soc.* **1998**, *120*, 5080−5085.
(32) Liu, A.; Pötsch, S.; Davydov, A.; Barra, A.-L.; Rubin, H.; Gräslund, A. *Biochemistry* **1998**, *37*, 16369−16377.
(33) (a) Nordlund, P.; Sjöberg, B.-M.; Eklund, H. *Nature* **1990**, *345*, 593−598. (b) Nordlund, P.; Eklund, H. *J. Mol. Biol.* **1993**, *232*, 123−164.
(34) Ormö, M.; Regenström, K.; Wang, Z.; Lawrence, Q.; Sahlin, M.; Sjöberg, B.-M. *J. Biol. Chem.* **1995**, *270*, 6570−6576.
(35) Fasanella, E. L.; Gordy, W. *Proc. Natl. Acad. Sci. U.S.A.* **1969**, *62*, 299−304.

catalase tyrosyl radical ($Tyr^{\bullet}_{CAT}$) was studied by high-field (285 GHz) EPR spectroscopy. Resonance Raman spectroscopy was used to study the protein electrostatic effect on an environmentally sensitive vibrational frequency, the C−O stretching mode (ν_{7a}) of the catalase tyrosyl radical. To analyze the experimental vibrational frequencies of the tyrosyl radical obtained from the RR measurements, we used *ab initio* hybrid density functional calculations. The *g* values obtained by HF-EPR measurements were analyzed using semiempirical MNDO calculations. To model the tyrosyl radicals in proteins, these calculations were performed on the water complexes of *p*-methylphenoxy and phenoxy radicals. Both types of calculations accurately reproduce the experimental *g* values and vibrational frequencies. In particular, the calculations predicted an unusual upshift of the vibrational frequency of the C−O stretching mode (ν_{7a}) for hydrogen bond distances larger than 1.7 Å, compared to the vibrational frequency observed for a non-hydrogen-bonded situation. Both the RR and the HF-EPR spectra of the $Tyr^{\bullet}_{CAT}$ showed a marked pH dependence for the pH range between 6.7 and 4.5. Our results argue for the presence of one or two hydrogen bond(s) to the $Tyr^{\bullet}_{CAT}$, and the observed pH dependence suggests the involvement of carboxylic groups and therefore favors aspartate or glutamate amino acid residues as candidates for hydrogen bond donation.

Materials and Methods

Sample Preparation. Bovine liver catalase (hydrogen peroxide: hydrogen peroxide oxidoreductase, EC 1.11.1.6; Boehringer Manheim) samples used for EPR and resonance Raman experiments were purified as previously described.[6] Samples of the catalase intermediate, used for the EPR and Raman experiments, were prepared by mixing quickly (15 s) native catalase with buffered solutions of peroxyacetic acid (Aldrich) and freezing by rapid immersion in liquid N_2. Samples with different final pH values were obtained by adjusting the pH of the peroxyacetic acid solution. All reported pH values correspond to those measured directly in the EPR tube immediately after thawing of the samples. Samples were prepared in an identical manner for EPR and RR measurements.

Resonance Raman Spectroscopy. Resonance Raman spectra were excited using the 406.7-nm line from a Kr^+ laser (Coherent Innova 90) or the 488.0-nm line from an Ar^+ laser (Coherent Innova 100). Measurements were performed at 15 K using a gas flow cryostat (SMC-TBT, France), regulated by circulation of cold helium gas. The scattered light was collected using a 130° grazing incidence geometry and dispersed through a U-1000 Jobin-Yvon Raman spectrometer equipped with a liquid nitrogen-cooled charge coupled device detector (Spectraview 2D, Jovin Yvon). Typically, less than 5 mW of laser power was measured at the cryostat window. Spectral resolution was 6 cm^{-1}. The reported spectra were the result of the average of four individual accumulations, each of 300-s exposures. For these experiments, native catalase samples of 0.75 μM ($\epsilon_{405} = 3.24 \times 10^5\ M^{-1}\ cm^{-1}$) were used. Comparative measurements were done by placing both the native and the peroxyacetic acid-treated catalase on the same sample holder in order to minimize possible geometry changes. The spectrometer was calibrated using the intense bands at 922 and 1377 cm^{-1} of frozen acetonitrile at 15 K as standards, resulting in an accuracy of 1 cm^{-1}.

The samples of the [(Fe(IV)═O)$Tyr^{\bullet}$] catalase intermediate contained small amounts of native catalase, as revealed by the X-band EPR spectrum. For the native catalase, the RR spectrum of the heme molecule excited at 406.7 nm is much better resonance enhanced via its Soret absorption band at 405 nm than the [(Fe(IV)═O)$Tyr^{\bullet}$] intermediate (Soret band at 430 nm). Accordingly, the presence of a low percentage of native catalase has a non-negligible contribution to the [(Fe(IV)═O)$Tyr^{\bullet}$] intermediate spectrum excited at 406.7 nm. For all the RR catalase intermediate spectra reported in this work, a percent (25% for the low-pH samples and 35% for the high pH-samples) of native catalase spectrum was subtracted, using the criterion of obtaining no negative bands. The same procedure has been used previously for RR spectra of compounds I and II of horseradish peroxidase (HRP).[36]

EPR Spectroscopy. Conventional 9-GHz EPR measurements were performed using a Bruker ER 200 spectrometer with a standard TE_{102} cavity equipped with a liquid helium cryostat (Oxford Instrument), a microwave frequency counter (Hewlett-Packard 5350B), and an NMR gaussmeter (Bruker ER035M). All samples used for the HF-EPR experiments were prepared just before the measurements, and 9-GHz EPR spectra were recorded before and after the high-field measurements. For all EPR experiments, native catalase samples of 0.25 μM ($\epsilon_{405} = 3.24 \times 10^5\ M^{-1}\ cm^{-1}$) were used. The HF-EPR spectra reported here were obtained under nonsaturating conditions. To obtain spectra with reasonable signal-to-noise ratios when using low microwave power, relatively large field modulation, 10 G, was necessary.

(i) High-Field (285 GHz) Spectrometer. The HF-EPR spectrometer followed the design of Muller and co-workers.[37] The microwave source was a Gunn-Diode (Epsilon-Lambda, Geneva, IL) with a range of 90−100 GHz and a maximum output power of 90 mW. The frequency was measured using a frequency counter (EIP Microwave Inc., Milpitas, CA) with a specified accuracy of better than 1 kHz. The frequency of the Gunn Diode was tripled using an InP frequency tripler (Radiometric Physics, Menkenheim, Germany). The maximum resulting power was 3 mW. Spectra were obtained using 50−750 μW. The microwave power absorbed by the sample was measured using a bolometer (QMC Instruments Ltd., United Kingdom) in conjunction with a lock-in amplifier (SRS, Sunnyvale, CA). The magnetic field was generated using a superconducting 10.5-T magnet (Oxford Instruments, Oxon, England). The value of the magnetic field was obtained from the magnet power supply, which had a manufacturer-specified accuracy of ±0.05 mT. The power supply calibration was corrected using an NMR gaussmeter and by EPR measurements using Mn(II) doped in magnesium oxide ($g = 2.00101$)[41] and Mn(II) concanavalin samples. Under conditions with which the data were obtained, the absolute field uncertainty was as large as ±1.0 mT, or about an error of 2×10^{-4} in *g*. It should be emphasized that the relative accuracy of the field measurements, that is, the uncertainty in the field difference between two data points of a given spectrum, was much smaller and typically only limited by the resolution of the data, 0.2−0.1 mT (2×10^5). The reproducibility of the *g* values for a given sample was less than 5×10^{-5}. Field modulation was used to detect the signal. The amplitude of field modulation was calibrated using the Mn(II) signal from a concanavalin sample, and uncertainty was estimated to be less than ±0.05 mT. Sample temperature regulation was achieved using a built-in helium flow cryostat. The accuracy of temperature at the sample was estimated to be ±0.2 K.

(ii) Simulations of the EPR Spectra. The HF-EPR powder patterns were simulated using locally written Fortran programs with standard numerical routines.[38] The *g*-tensor and the distribution in *g* values (see below) were taken into account in the simulations. Hyperfine couplings were not explicitly considered in the simulations, as no resolved hyperfine couplings were observed. The distribution in *g* values was treated as tensor quantity, the principal axes of which were collinear with the *g*-tensor. A Gaussian distribution in the *g* values was assumed. A calculated spectrum was generated in the following manner. One million random orientations of the magnetic field with respect to the

(36) Ogura, T.; Kitagawa, T. *J. Am. Chem. Soc.* **1987**, *109*, 2177−2179.
(37) Muller, F.; Hopkins, M. A.; Coron, N.; Grynberg, M.; Brunel, L.; Martinez, G. *Rev. Sci. Instrum.* **1989**, *60*, 3681−3684.
(38) Press, W. H.; Flannery, B. P.; Teukolsky, S. A.; Vetterling, W. T. *Numerical Recipes*; Cambridge University Press: New York, 1986.
(39) Stewart, J. J. P. MOPAC, A Semiempirical Molecular Orbital Program. *QCPE* **1983**, 455.
(40) Frisch, M. J.; Trucks, G. W.; Schlegel, H. B.; Gill, P. M. W.; Johnson, B. G.; Robb, M. A.; Cheeseman, J. R.; Keith, T.; Petersson, G. A.; Montgomery, J. A.; Raghavachari, K.; Al-Laham, M. A.; Zakrzewski, V. G.; Ortiz, J. V.; Foresman, J. B.; Cioslowski, B. B.; Stefanov, B. B.; Nanayakkara, A.; Challacombe, M.; Peng, C. Y.; Ayala, P. Y.; Chen, W.; Wong, M. W.; Andres, J. L.; Reploge, E. S.; Gomperts, R.; Martin, R. L.; Fox, D. J.; Binkley, J. S.; Defrees, D. J.; Baker, J.; Stewart, J. P.; Head-Gordon, M.; Gonzalez, C.; Pople, J. A. *Gaussian 94*, Revision D.2; Gaussian Inc.: Pittsburgh, PA, 1995.
(41) Burghaus, O.; Rohrer, M.; Götzinger, T.; Plato, M.; Möbius, K. *Meas. Sci. Technol.* **1992**, *3*, 765−774.

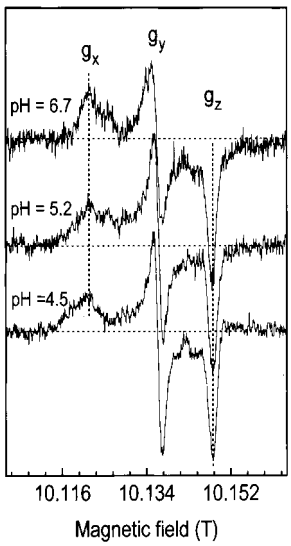

Figure 1. High-field (10 T, 285 GHz) EPR spectra of the catalase tyrosyl radical at pH values of 6.7, 5.2, and 4.5. Spectra were recorded at 30 K and under nonsaturating conditions. A field modulation of 10 G and a frequency modulation of 30 kHz were used. Each spectrum was recorded at slightly different microwave frequencies (284.54, 284.35, and 283.72 GHz). For comparison, the three spectra are aligned to a nominal field.

principal axis system of the *g*-tensor were chosen. To obtain a Gaussian distribution of the *g* values along the three principal directions, a Gaussian deviant random number generator was used to obtain three numbers which described the deviations in *g* values along each of the three directions. For each randomly chosen orientation, the three numbers were appropriately scaled and added to the nominal *g* values and the resonant field was calculated for the particular orientation. The powder pattern was generated by summing the results of all the orientations, followed by a Fourier convolution with the derivative of a Gaussian function, yielding a derivative line shape suitable for comparison to the experimental data. The calculated spectrum was scaled to the experimental spectrum using a scaling factor obtained from a linear fit of 10−20 data points. Aside from this global scaling factor, the calculation of the powder spectrum required seven parameters: three *g* values, three values for extent of Gaussian distribution, and a global line width. Conjugate gradient minimization was used to obtain "best-fit parameters".[38]

Molecular Orbital Calculations. All semiempirical molecular orbital calculations were carried out using a modified version of MOPAC 6.0.[39] As previously described, the modifications were nonsubstantial and facilitated subsequent *g* values.[13] The MNDO-based *g* value calculations have been previously described. The *ab initio* hybrid Hartree−Fock density functional calculations were done using Gaussian 94 (revision D.2).[40] All molecular orbital calculations as well as the simulations were performed on either an Alphastation 255 or 600au (DEC, Maynard, MA).

Results

High-Field (285 GHz) EPR Spectrum of the Catalase Tyrosyl Radical: pH Dependence. Figure 1 shows the 30 K HF-EPR spectra of the catalase tyrosyl radical ($Tyr^{\bullet}_{CAT}$) at three different pH values. The envelope of the spectrum is dominated by *g*-anisotropy and shows no resolved hyperfine coupling pattern. Subsequent experiments at 95, 190, and 285 GHz showed that all the observed features at 285 GHz scaled with microwave frequency. The field positions of the three readily observed features in each spectrum correspond to principal *g* values. The orientation of the *g*-tensor of the radical was taken as that of the γ-irradiated Tyr-HCl crystal.[35] It has been shown previously that the g_x component (C−O bond direction) is strongly dependent on the local protein environment of the radical, the g_y component reflects protein effects but to a lesser extent, with an approximate value of 2.0045, and the g_z component (perpendicular to the phenol ring) is largely invariant for all tyrosyl radicals, with a value of approximately 2.00212.[13] The *g* values obtained from the simulations which best reproduce the powder pattern spectra of the $Tyr^{\bullet}_{CAT}$ at three different pH values ranging from 6.7 to 4.5 (Figure 1) are listed in Table 1. As with other tyrosyl radicals, the g_y and g_z components of the catalase $Tyr^{\bullet}$ exhibit approximate values of 2.00450 and 2.00210, respectively, for all pH values (Figure 1). The g_x component exhibits an approximate value of 2.00740 at pH 6.7, with a measurable shift to 2.00760 for pH values $\leq$4.5 (Figure 2A). The overall line shape of the g_x edge of the $Tyr^{\bullet}_{CAT}$ spectrum appears to be pH dependent as well. No measurable change in the line width of the g_x edge was observed over a temperature range from 4 to 40 K (data not shown).

The low-field edge, g_x component, of the catalase tyrosyl radical HF-EPR spectrum was broad for all samples regardless of the pH, as compared to that of the PSII $Tyr^{\bullet}_{D}$ ($Tyr^{\bullet}_{PSII-D}$) or the RNR $Tyr^{\bullet}$ ($Tyr^{\bullet}_{RNR}$) (see Figure 2 in ref 13). The spectral simulations which best reproduce the actual broadness of the $Tyr^{\bullet}_{CAT}$ spectra were those assuming an isotropic line width of 10 G, and Gaussian widths of 0.00047 (pH 6.7), 0.00060 (pH 5.2), and 0.00067 (pH 4.5) along the g_x direction, and no distribution in g_y and g_z. For the $Tyr^{\bullet}_{PSII-Z}$, a g_x distribution of 0.0007 (approximately 30 G at 10 T) was required for the spectral simulations, while no anisotropic distribution was necessary for $Tyr^{\bullet}_{PSII-D}$.[27] The broadness of the g_x edge in the HF-EPR spectrum of the $Tyr^{\bullet}_{PSII-Z}$, as compared to that of $Tyr^{\bullet}_{PSII-D}$, was attributed to a distribution in hydrogen bond strengths.

The distribution in g_x values was different for each $Tyr^{\bullet}_{CAT}$ spectrum taken at different pH values and distinct from that of $Tyr^{\bullet}_{PSII-Z}$. A detailed comparison of line shapes of the $Tyr^{\bullet}_{CAT}$ g_x edge at the three different pH values (Figure 2A) to that of the $Tyr^{\bullet}_{PSII-Z}$ (see Figure 2 in ref 13) revealed a difference in their distributions. In particular, while the spectrum of $Tyr^{\bullet}_{PSII-Z}$ was characterized by a single Gaussian distribution centered at 2.00750, the line shapes of the $Tyr^{\bullet}_{CAT}$ spectra were asymmetric. The shape of the $Tyr^{\bullet}_{CAT}$ spectrum could be pictured as arising from two contributions whose maxima are pH dependent (Figure 2A). At pH = 6.7, the maximum of the g_x is at 2.0073(8), with a distinguishable feature at 2.0065(5). At pH 4.5, the maximum was significantly shifted to 2.0076(2), with a distinguishable feature at 2.0082(4). The intermediate pH sample (pH 5.2) was very similar to the higher pH spectrum, with an additional, although minor, feature at 2.0082(4). The g_x values of the minor features on the high- and low-pH spectra of the $Tyr^{\bullet}_{CAT}$ are similar in magnitude to the reported g_x values of the tyrosyl radicals in the Tyr-HCl crystals (2.00670) and RNR (2.00866) (see Table 1).

The HF-EPR spectra of the catalase $Tyr^{\bullet}$ at pH above 5.2 were identical to that at pH 6.7, and those spectra between pH 5.2 and 4.5 were identical to that at pH 4.5 (data not shown). At pH values below 4.0, the enzyme precipitated. The 9-GHz EPR spectra of the radical at different pH values (data not shown) were essentially identical to that reported previously for pH of 5.6 (see Figure 1B in ref 6). This result is expected since the g_x distribution observed in the HF (285 GHz) EPR spectrum of the catalase $Tyr^{\bullet}$ scales to less than 2 G at 9 GHz, a value that is below the inhomogeneous line width and thus would be difficult to detect in the X-band EPR spectrum.

Table 1. Comparison of g Values, g-Anisotropy, and ν_{7A} Vibrational Frequency of the Catalase Tyrosyl Radical with Those of Ribonucleotide Reductase and Photosystem II

	ν_{7a}(C−O)[j]	ν_{7a} line width[j]	g_x	g_y	g_z	Δg[k]
cat Tyr• (pH = 6.7)[a]	1484 (RR)	9	2.0073(8)	2.0044(4)	2.0020(9)	0.00529
(minor fraction)			(2.0065(5))			(0.00446)
cat Tyr• (pH = 5.2)[a]	1484 (RR)	9	2.0073(9)	2.0043(8)	2.0020(9)	0.00530
(minor fraction)			(2.0065(5))			(0.00446)
cat Tyr• (pH = 4.5)[a]	1488 (RR)	16	2.0076(2)	2.0044(2)	2.0020(9)	0.00563
(minor fraction)			(2.0082(4))			(0.00615)
Tyr• (HCl)[b]	nd	nd	2.0067	2.0042	2.0023	0.0044
PSII $Tyr^{\bullet}_D$	1503 (IR)[c]	9[c]	2.0074(0)[d]	2.0042(5)[d]	2.0020(5)[d]	0.00535
PSII $Tyr^{\bullet}_Z$	1513 (IR)[c]	13[c]	2.0075(0)[d]	2.0042(2)[d]	2.0022(5)[d]	0.00523
mouse and HSV1 RNR Tyr•	nd	nd	2.0076[e,f]	2.0043[e,f]	2.0022[e,f]	0.0054
E. coli RNR Tyr•	1498 (RR)[g]	10[g]	2.0086(6)[h]	2.0042(3)[h]	2.0020(0)[h]	0.00666
			2.0091(2)[i]	2.0045(7)[i]	2.0022(5)[i]	0.00687

[a] Bovine liver catalase, this work. [b] Tyrosine hydrochloride γ-irradiated crystals, from ref 35. [c] *Synechocystis* PSII, from ref 22. [d] *Synechocystis* PSII, from ref 27. [e] Herpes simplex virus, from ref 31. [f] Mouse RNR, from ref 30. [g] *E. coli* RNR, from ref 15. [h] *E. coli* RNR, from ref 13. [i] *E. coli* RNR, from ref 28. [j] FWMH, in cm^{-1}. [k] $\Delta g = |g_x - g_z|$.

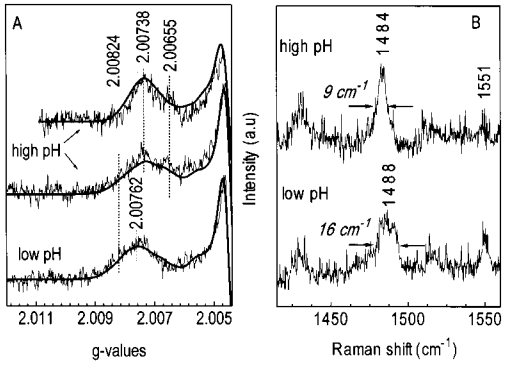

Figure 2. (A) g_x edges of the experimental high-field (285 GHz) EPR spectra of the catalase tyrosyl radical for high (6.7 and 5.2) and low (4.5) pH values, together with their simulation (solid line). The dotted bars show the g_x values obtained from the simulation of the spectra (2.00738 and 2.00762), taking an isotropic line width of 10 G and a distribution in g_x values (see Results). The observed g_x values for the minor features observed in each spectra are also shown by dotted bars. (B) The 1450−1550-cm^{-1} region of the 15 K resonance Raman spectra of the [(Fe(IV)═O) Tyr•] catalase intermediate, excited at 406.7 nm, for the high and low pH values. The arrows show the broadening of the 1484-cm^{-1} band assigned to the C−O stretching mode (ν_{7a}) of the tyrosyl radical, as measured by the changes in line width (see Table 1).

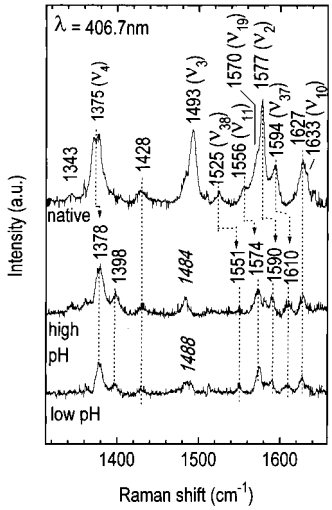

Figure 3. 15 K resonance Raman spectra, excited at 406.7 nm, of native catalase (top) and the [(Fe(IV)═O) Tyr•] catalase intermediate at high and low pH values (middle and bottom, respectively), for the spectral region between 1310 and 1660 cm^{-1}. The arrows show the shift to higher vibrational frequencies of the bands assigned to the porphyrin modes upon the two-electron oxidation of the native ferric catalase.

Resonance Raman Spectrum of the [(Fe(IV)═O)Tyr•] Catalase Intermediate. Figure 3 shows the 1310−1660-cm^{-1} spectral region of the 15 K resonance Raman spectra of ferric (native) catalase together with the tyrosyl intermediate at two different pH values, all excited at 406.7 nm. This spectral region includes the porphyrin marker bands corresponding to vibrational modes that are very sensitive to changes in the coordination number, as well as the oxidation and spin states of iron in the heme molecule (for reviews, see refs 42 and 43). The resonance Raman spectra of ferric catalase and those of the [(Fe(IV)═O) $por^{\bullet+}$] and [Fe(IV)═O] intermediate states (so-called compound I and compound II, respectively) were characterized previously by resonance Raman spectroscopy using various excitation wavelengths.[45−47] The 406.7-nm wavelength used in the present study excites preferentially the polarized modes of the heme group in its ferric state via the Soret electronic absorption band (see Figure 3B in ref 6). Moreover, such a wavelength is also convenient in exciting the resonance Raman spectrum of tyrosyl radicals whose absorption bands are typically at 410 nm.[15,18]

The bands of the native catalase RR spectrum (Figure 3, top) observed at 1375, 1493, 1525, 1556, 1570, 1577, 1594, and 1633 cm^{-1} were those previously assigned to the vibrational frequencies of the porphyrin modes ν_4, ν_3, ν_{38}, ν_{11}, ν_{19},ν_2, ν_{37}, and ν_{10}, respectively.[44] The minor differences in vibrational frequencies and line widths of the porphyrin marker bands as compared to the previously reported spectra were due to the different temperatures at which spectra were recorded. The bands observed at 1343, 1428, and 1626 cm^{-1} in the native catalase spectrum were those of vinyl modes.[44] The ν_4 mode, a characteristic marker band for the heme iron oxidation state, is typically observed in the range 1368−1376 cm^{-1} for ferric hemes.[42] The bands corresponding to the ν_3 and ν_{10} modes are diagnostic for the spin-state and ligation of the iron in the

(42) Spiro, T. G. In *Iron Porphyrins Part II*; Lever, A. B. P., Gray, H. B., Eds.; Addison-Wesley Publishing Co.: Reading, MA, 1983.
(43) Kitagawa, T.; Mizutani, Y. *Coord. Chem. Rev.* **1994**, *135/136*, 685−735.
(44) Sharma, K. D.; Andersson, L. A.; Loehr, T. M.; Terner, J.; Goff, H. M. *J. Biol. Chem.* **1989**, *264*, 12772−12779.
(45) Chuang, W.-J.; Van Wart, H. E. *J. Biol. Chem.* **1992**, *267*, 13293−13301.
(46) Chuang, W.-J.; Heldt, J.; Van Wart, H. E. *J. Biol. Chem.* **1989**, *264*, 14209−14215.
(47) Johnson, C. R.; Ludwig, M.; Asher, S. A. *J. Am. Chem. Soc.* **1986**, *108*, 905−912.

porphyrin molecule. In particular, for high-spin ferric hemes, ν_3 is normally observed in the range of 1478−1494 cm^{-1} and ν_{10} at 1605−1626 cm^{-1}. For pentacoordinated high-spin ferric hemes, ν_3 is observed in the spectral range of 1487−1494 cm^{-1}.[42] Therefore, the porphyrin marker bands in the native catalase spectrum of Figure 3 (top) were those of a high-spin pentacoordinated ferric heme. The shoulder observed in the low-frequency side of the 1493 cm^{-1} band could arise from a fraction of (high-spin) hexacoordinated heme molecules.

The [(Fe(IV)═O)Tyr•] catalase intermediate formed by the reaction with an excess of peroxyacetic acid exhibited an electronic absorption spectrum typical of an oxoferryl species [Fe(IV)═O] and EPR and ENDOR spectra typical of a tyrosyl radical.[6] Thus, the RR spectrum of such an intermediate is expected to be that of the compound II species [Fe(IV)═O],[46] with additional bands corresponding to the tyrosyl radical vibrational frequencies,[15,47] if the Tyr• can be sufficiently resonance enhanced by using an appropriate excitation wavelength. It has been shown that all the porphyrin marker bands, which are sensitive to the iron oxidation and spin state as well as coordination number, upshift between 2 and 25 cm^{-1} upon compound II formation (see Table 1 in ref 46). For example, the ν_4 mode has been observed to upshift between 2 and 4 cm^{-1} when ferric horseradish peroxidase (HRP) and cytochrome *c* peroxidase (CCP) are converted to the compound II and compound ES [(Fe(IV)═O) Trp•] intermediates, respectively.[48,49] The ν_3 band has been reported to upshift 14 cm^{-1} for CCP upon conversion to compound ES[49] and 26 cm^{-1} for catalase compound II.[46] In contrast, the bands assigned to the porphyrin vinyl modes in these proteins remained essentially unchanged.[46]

Figure 3 (middle and bottom) shows the RR spectra of the [(Fe(IV)═O)Tyr•] intermediate at two different pH values. The predominant band observed at 1378 cm^{-1} is assigned to the ν_4 mode that upshifted from 1375 cm^{-1} in the ferric catalase RR spectrum due to the change in the iron oxidation state. Accordingly, the 1525- (ν_{38}), 1556- (ν_{11}), 1570- (ν_{19}), 1577- (ν_2), and 1594-cm^{-1} (ν_{37}) bands of the ferric catalase upshifted to 1551, 1574, 1580, 1590, and 1610 cm^{-1}, respectively, upon conversion from the high-spin pentacoordinated ferric species to the low-spin hexacoordinated oxoferryl species. The bands assigned to the vinyl modes were those observed at 1343, 1428, and 1627 cm^{-1} in both the native and the intermediate catalase spectra. The 1493-cm^{-1} (ν_3) band of native catalase is expected to upshift to approximately 1520 cm^{-1} upon formation of the [(Fe(IV)═O)Tyr•] intermediate (see above). The apparent absence of such a band in the RR spectra of Figure 3 (middle and bottom) is due to its unfortunate overlap with the 1525-cm^{-1} band (ν_{38}) of the native catalase, both bands canceling out in the subtraction (see Materials and Methods). The 1633-cm^{-1} band (ν_{10}), which is expected to upshift to approximately 1646 cm^{-1} (see above), is extremely weak in the spectra of Figure 2 (middle and bottom). However, this mode is clearly observed when using a 488.0-nm excitation wavelength (data not shown). For all previously reported compound II RR spectra excited at 406.7 nm (HRP, CCP, catalase), the bands observed in the 1570−1600-cm^{-1} spectral region showed very similar relative intensities.[46,48,49] In contrast, in the spectra of Figure 3 (middle and bottom), the band at 1574 cm^{-1} is significantly more intense than the 1580- and 1590-cm^{-1} bands. A possible explanation for the unusual intensity of the 1574-cm^{-1} band is the contribution of an additional, non-porphyrin mode (see below).

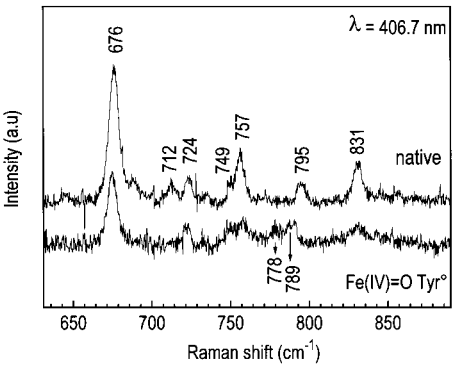

Figure 4. Low-frequency region of the 15 K resonance Raman spectra of the native (top) and [(Fe(IV)═O) Tyr•] intermediate (bottom) species of catalase. Experimental conditions are the same as those of Figure 3.

Figure 4 shows the 630−900-cm^{-1} spectral region of native catalase and its [(Fe(IV)═O)Tyr•] intermediate. The broad band observed at approximately 780 cm^{-1} in the spectrum of the catalase intermediate species is consistent with that of the Fe-(IV)═O stretching mode of HRP, CCP, and catalase compound II, for which oxygen labeling experiments confirmed the origin of this mode (for a review, see ref 43). It has been shown that the vibrational frequency of the Fe═O mode of catalase compound II is sensitive to pH changes.[46] As the pH was increased from 7.0 to 8.9, the band assigned to the ν(Fe═O) mode observed at 775 cm^{-1} (pH 7.0) decreased in intensity and was replaced by a new band at 789 cm^{-1} (pH 8.9). Moreover, both bands were observed at pH 7.9. Similarly, the broadness observed for the band centered at 780 cm^{-1} in the catalase intermediate spectrum of Figure 4 may be indicative of a contribution of two different pH forms.

The above analysis leaves the 1484-cm^{-1} band unaccounted for in the catalase [(Fe(IV)═O)Tyr•] intermediate spectrum (Figure 3, middle). No band corresponding to the porphyrin modes is expected to upshift to a vibrational frequency of about 1484 cm^{-1} upon formation of the catalase compound II species.[46] In the native catalase spectrum, a band at approximately 1484 cm^{-1} is observed as a shoulder on the ν_3 band (1593 cm^{-1}), but it could not be the same band as that observed in the [(Fe(IV)═O)Tyr•] spectrum, because all the contributions from the native catalase were subtracted (see Materials and Methods). Other possible species from which this band may be arising are the acetic and/or peroxyacetic acids present in the sample. The Raman spectra for both acids, recorded under the same conditions as those of Figure 3, exhibited extremely weak bands at 1432 and 1467 cm^{-1} (data not shown) but no band at 1484 cm^{-1}. Moreover, when 488-nm excitation was used, such a band was not observed in the RR spectrum (data not shown). Therefore, the 1484-cm^{-1} band in the [(Fe(IV)═O) Tyr•] catalase intermediate spectrum was a new non-porphyrin band which had been resonance enhanced at 406.7 nm. Taking into account that the catalase intermediate species is composed of an oxoferryl moiety and a tyrosyl radical (see above), and that tyrosyl radicals have sizable absorption at approximately 410 nm, the $Tyr^{\bullet}_{CAT}$ species should be enhanced to a significant degree in the spectrum of Figure 3 (middle). The vibrational frequency of the new band observed in the [(Fe(IV)═O) Tyr•] intermediate RR spectrum is in a reasonable range for the C−O stretching mode (ν_{7a}) of a tyrosyl radical.[15] Consequently, we assigned the 1484-cm^{-1} band to the ν_{7a} mode of the $Tyr^{\bullet}_{CAT}$.

(48) Teraoka, J.; Ogura, T.; Kitagawa, T. *J. Am. Chem. Soc.* **1982**, *104*, 7354−7356.
(49) Hashimoto, S.; Teraoka, J.; Inubushi, T.; Yoetani, T.; Kitagawa, T. *J. Biol. Chem.* **1986**, *261*, 11110−11118.

Based on results from *in vitro* phenoxyl and tyrosyl radicals, the ν_{8a}(C−C) stretching mode can be observed at 1577 cm^{-1}.[47] This mode is not strongly enhanced by the 406.7-nm excitation;[50] thus, a weak band[47] could be expected in the RR spectrum of the [(Fe(IV)═O) Tyr•] intermediate. It was stated before that the additional intensity observed for the 1574-cm^{-1} porphyrin band (ν_{11}) originates from the contribution of a non-porphyrin mode. Such a vibrational frequency is well within the range expected for the ν_{8a} mode of a tyrosyl radical, and we tentatively assigned this band to the $Tyr^{\bullet}_{CAT}$ (C−C) stretching mode (ν_{8a}).

While all other bands in the [(Fe(IV)═O)Tyr•] intermediate spectrum showed no measurable changes with pH, a remarkable effect on the band assigned to the $Tyr^{\bullet}_{CAT}$(C−O) stretching mode was observed (Figure 2B). This band, observed at 1484 cm^{-1} in the high-pH spectrum, upshifts to 1488 cm^{-1} at low pH values. Moreover, it becomes considerably broader (16 cm^{-1} fwhm) at low pH as compared to its line width at high pH (9 cm^{-1} fwhm). A corresponding behavior was observed for the g_x value (the g value in the C−O bond direction) in the HF-EPR spectrum (see previous section).

Hybrid Density Functional Calculations. The BPW91 (Perdew-Wang 91[51]) density functional calculations using Gaussian 94 with the 6-31G** and 6-31G* basis sets were carried out to investigate the effect of hydrogen bonding on the vibrational frequencies of the tyrosyl radical. Zhan and Chipman[52] have shown that the vibrational frequencies for water−benzosemiquinone clusters calculated at the same level of accuracy reproduce the experimental frequencies.[53] Normal modes have also been calculated for isolated phenoxy radicals[23,54] using the B3LYP (Beck−Lee−Yang−Parr) density functionals and 6-31* basis set. Following the approach of Zhan and Chipman,[52] we calculated the vibrational frequencies of *p*-methylphenoxy hydrogen-bonded by one water molecule and phenoxy radicals in the presence of one and two water molecules using the BPW91 density functionals with 6-31G* and 6-31G** basis sets.[55] The vibrational frequencies were calculated as a function of the distance between the phenoxy (or *p*-methylphenoxy) oxygen and one of the proton of the water molecules.

(i) Optimized Geometries. The 6-31G* and 6-31G** geometry-optimized structures of the isolated *p*-methylphenoxy were identical, as were the two optimized structures obtained for the isolated phenoxy radical. However, the BPW91 density functional method used in this study yielded *p*-methylphenoxy bond lengths that were different from those obtained in previous studies using B3LYP.[23,54,56] The BPW91 method yielded bond lengths that were 0.005−0.009 Å longer. The most important difference was the length of the C−O bond. The BPW91 distance was 1.264 Å, as compared to the B3LYP distance of 1.257 Å, both for 6-31G* and 6-31G** basis sets.

For the *p*-methylphenoxy water complex, the (C)O···H···O angle steadily decreased from 172° for O···H distance of 1.45 Å to 166° at 1.80 Å. The C−O···H bond angle and dihedral angle relative to the phenyl ring plane were independent of the hydrogen-bonding distance with values of (112 ± 1)° and (3 ± 1)°, respectively. Essentially, the same results were obtained for the one-water phenoxy radical complex. For the two-water-phenoxy radical complex, the C−O···H bond angle was marginally larger, at 113°. The geometry of the water molecules was identical to that describe by Zhan and Chipman[52] in their study of benzosemiquinone−water complexes. The presence of a single water molecule at a distance of 3.0 Å yielded a C−O bond length of 1.273 Å and an elongation of 0.009 Å as compared to the isolated radical. Apparently, the C−O bond length is very sensitive to the presence of the hydrogen bond donor. The rest of the *p*-methylphenoxy structure exhibited smaller changes in bond lengths (less than 0.005 Å) compared to the isolated radical. The dependence of the C−O bond length on the hydrogen bond distance is shown in Figure 5A, along with the corresponding total BPW91/6-31G* energies (Figure 5B). At hydrogen bond distance of less than 2 Å, the C−O bond length steadily decreases, reaching a value of 1.271 Å, and thereafter rises sharply. The extent of change, 0.007 Å, in the C−O bond length compared to the isolated radical is identical to that calculated for a benzosemiquinone−water complex.[52] The total energy of the *p*-methylphenoxy−water complex exhibited the same functional dependence as the C−O bond length. Relative to the 3-Å case, the complex becomes destabilized when the hydrogen-bonding distance is less than 1.70 Å. Contrary to simple expectations and unlike the semiquinone−water complexes calculated by Zhen and Chipman,[52] the BPW91/6-31G* calculations indicate that hydrogen bonding results in contraction of the C−O bond rather than in elongation for hydrogen bond distances larger than 1.7 Å. As will be discussed, this prediction is, in fact, supported by the experimental vibrational data.

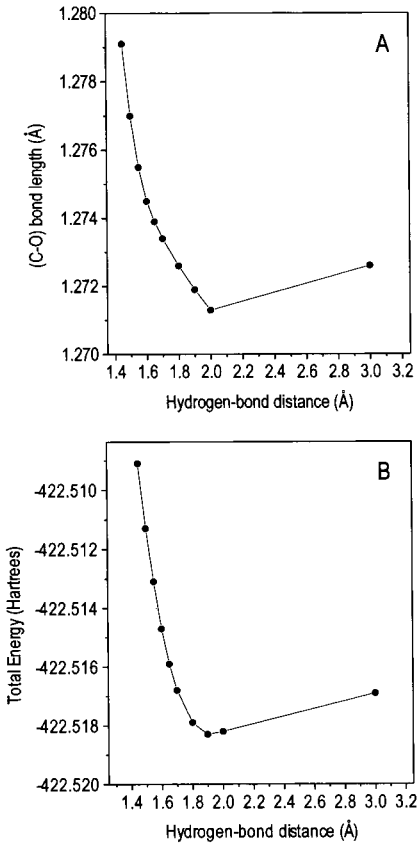

Figure 5. Calculated dependence of the C−O bond length (A) and the total energy (B) of the *p*-methylphenoxy radical as a function of the hydrogen bond distance to a single water molecule.

(ii) Calculations of Vibrational Modes. The vibrational frequencies of the *p*-methylphenoxy−water complex were calculated for a series of hydrogen bond lengths using BPW91/

(50) Tripathi, G. N. R.; Schuler, R. H. *J. Phys. Chem.* **1988**, *92*, 5129−5133.
(51) Perdew, J. P.; Wang, Y. *Phys. Rev. B* **1992**, *45*, 13244−13249.
(52) Zhan, C.-G.; Chipman, D. *J. Phys. Chem. A* **1998**, *102*, 130−1235.
(53) Qin, Y.; Wheeler, R. A. *J. Am. Chem. Soc.* **1995**, *117*, 6083−6092.
(54) Adamo, C.; Subra, R.; Di Matteo, A.; Barone, V. *J. Chem. Phys.* **1998**, *109*, 10244−10254.
(55) The *p*-methyphenoxy−two-water complex was not calculated due to lack of computational resources.
(56) Un, unpublished results.

Table 2. Comparison of Vibrational Frequencies (cm^{-1}) of Calculated and Experimental Selected Modes for *p*-methylphenoxy and Phenoxy Radicals Complexed with Water(s)

p-Methylphenoxy Radical				
Wilson mode[a]	in vitro[b]	in vivo	BPW91/ 6-31G**	BPW91/ 6-31G*
ν_{7a}(C−O)	1517	1498[c] (1503)[d]	1496	1498 (1503)[e]
ν_{8a}(C−C)	1577	nd	1581	1586
ν_{19a} (C−C)	1407	nd	1411	1405

Phenoxy Radical Complexed with One and Two Water(s) at 1.7 Å				
	in vitro	BPW91/	BPW91/6-31G*	
Wilson mode[a]	(expt)[g]	6-31G**	one H_2O	two H_2O
ν_{7a}(C−O)	1505	1483	1487	1485
ν_{8a}(C−C)	1552	1563	1572	1577
ν_{19a}(C−C)	1398	1417	1420	1418
ν_{9a}(C−H)	1157	1144	1159	1168
ν_1	840	787	795	797
ν_{6a}(C−C−C)	528	513	518	516

[a] Defined in ref 73. [b] From refs 18 and 50. [c] RNR $Tyr^{\bullet}_{122}$, from ref 15. [d] *Synechocystis* PSII $Tyr^{\bullet}_{D}$, from ref 22. [e] One-water−*p*-methylphenoxy radical complex with $O_{phenol}\cdots H_{water}$ distance of 1.7 Å.

6-31G*. The normal modes of the complex corresponding to those of the isolated system labeled ν_{7a}, ν_{8a}, and ν_{19a} were readily identifiable. The calculated frequencies of isolated *p*-methylphenoxy are listed in Table 2, along with frequencies of the complex at a hydrogen bond distance of 1.7 Å. As with the semiquinone water complexes, the BPW91/6-31G* and BPW91/6-31G** hybrid density functionals yielded frequencies that were in good agreement with experimental values. The calculated ν_{8a} and ν_{19a} frequencies were within 9 and 4 cm^{-1}, respectively, of the experimental values, depending on the level of the calculations and whether water molecules were included. The calculations were in good agreement with the vibrational frequency of the ν_{7a} mode observed for the tyrosyl radical in ribonucleotide reductase.[15] The crystallographic structure of RNR has been determined, and it is known that the tyrosyl radical resides in a hydrophobic pocket and is not hydrogen bonded.[33,34] In contrast, all *in vitro* studies, including the work of Tripathi and Schuler[18,50] listed in Table 2, involved radicals in aqueous solution under basic conditions, in the presence of salt ions, and hence were likely to be hydrogen bonded. The calculated frequencies of the unsubstituted phenoxy radical are in good agreement with the experimental values. The calculated ν_{8a} and ν_{19a} modes were 20 cm^{-1} higher than the experimentally obtained values. This result is slightly better than those obtained using B3LYP/6-31G*. The ν_{9a}, ν_{6a}, and ν_1 modes were within 10 cm^{-1}. As shown in Table 2, the ν_{7a} is underestimated (−20 cm^{-1}) by the BPW91/6-31G* calculations for a fixed distance of 1.7 Å. The dependence of ν_{7a} frequencies of the *p*-methylphenoxy radical and phenoxy radicals as a function of hydrogen-bonding distance is shown in Figure 6 (top). The calculated frequencies clearly reflect the variations in C−O bond lengths (Figure 5A). As expected from the C−O bond length results, and unlike the semiquinones, the C−O vibrational frequency increases with decreasing hydrogen-bonding distances larger than 1.7 Å. The effect of the methyl group is essentially independent of the hydrogen bond distance, shifting the frequency of the ν_{7a} mode by 14 cm^{-1} for the one-water complex. An identical shift is expected for the two-water complex. Also shown in Figure 6 are the semiempirical MNDO calculations of the *g* values for the *p*-methylphenoxy water

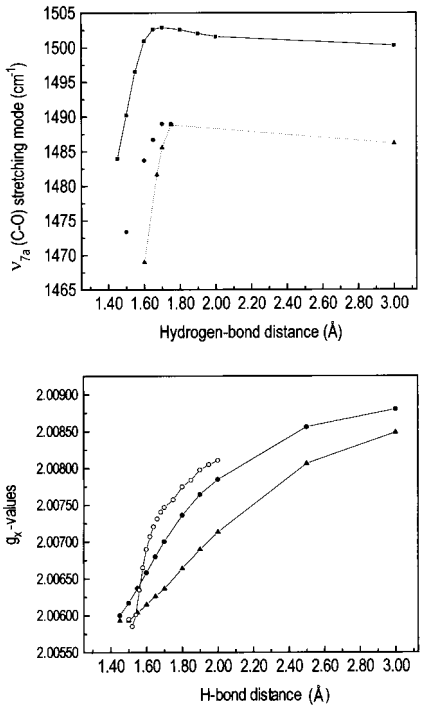

Figure 6. (Top) Variation of the ν_{7a}(C−O) stretching mode of the *p*-methylphenoxy (solid line with squares) and phenoxy (dotted line with triangles) radicals as a function of the hydrogen bond distance to one water molecule. The influence of a second water molecule on the ν_{7a} vibrational frequencies of the phenoxy radical is shown by some representative points (circles) in the turning point region. (Bottom) Semiempirical MNDO calculations on the variation of the g_x values (the *g*-tensor component in the direction of the C−O bond) of the *p*-methylphenoxy radical as a function of the hydrogen bond distance to one (solid line with circles) and two (solid line with triangles) water molecules. The effect of an acetic acid molecule as hydrogen bond donor to the *p*-methylphenoxy radical is shown as well[13] (open circles with dotted line).

complex using a C−O bond length of 1.25 Å.[57] This bond length is more consistent with the B3LYP/6-31G*-optimized structures and yields the best *g* values. The computed g_x for the *p*-methylphenoxy radical complexed with an acetic acid molecule[13] is also shown in Figure 6 (bottom).

Discussion

The *g* Values for the Catalase Tyrosyl Radical. The g_x values reported for the tyrosyl radicals in RNR, PSII, catalase, and Tyr-HCl crystals[5,13,26−32,35] are significantly different, with variations in the range of approximately 2.0090 to 2.0067. The reported g_x value for *E. coli* RNR is the highest observed thus far for tyrosyl radicals (Table 1). Such a value has been attributed to a radical which is electrostatically isolated with only a very weak interaction to the nearby metal active site.[13] The three-dimensional crystal structure of *E. coli* RNR revealed that Tyr_{122}, the site of the radical, is in a hydrophobic pocket with no amino acid residue that could act as hydrogen bond donor to the tyrosine residue. The Tyr_{122} is 5.2 Å away from the binuclear iron active site.[33,34,58] A different situation is found for the Tyr-HCl crystals. Neutron diffraction data showed that the phenol oxygen of each tyrosine is 1.6 Å away from the

(57) These results vary slightly from those previously published,[13] which used *p*-methylphenoxy acetic acid complex.

(58) The overall charge of the metal site is neutral, and hence the site interacts only weakly with the radical. For this reason, the observed *g* value of the $Tyr^{\bullet}_{RNR}$ is nearly equal to the calculated value for isolated *p*-methylphenoxy radical.

protonated carboxylic group of a neighboring tyrosine, and consequently all tyrosines are expected to be strongly hydrogen bonded.[59] The corresponding g_x value reported for the radical formed by γ-irradiation of the Tyr-HCl crystals ($Tyr^{\bullet}_{HCl}$) is 2.0067.[60] This low g_x value has been correlated to a strong hydrogen bond interaction to the $Tyr^{\bullet}_{HCl}$. The lower g_x value arises from the decrease in the energy of the nonbonding orbitals due to hydrogen bonding, which results in an increment of the energy difference between the nonbonding orbital and the SOMO ($\pi \rightarrow \pi^*$), and a decrease in the spin−orbit coupling contribution to the *g*-anisotropy.[13]

Comparison of the *g*-anisotropy of the catalase tyrosyl radical with those of *E. coli* RNR and Tyr-HCl crystals shows interesting differences (Table 1). The *g*-anisotropy, defined as $\Delta g = |g_x - g_z|$, for the $Tyr^{\bullet}_{CAT}$ is 0.00529 at pH = 6.7 and increases significantly to 0.00563 at pH = 4.5 (see Table 1). In both cases, the *g*-anisotropy in catalase (and thus the g_x value) is smaller than that observed for the *E. coli* RNR Tyr• (0.00666). We interpret this difference as arising from the presence of at least one hydrogen bond to the catalase tyrosyl radical. The fact that, for all pH values studied, the *g*-anisotropy of the $Tyr^{\bullet}_{CAT}$ is larger in magnitude than that of the $Tyr^{\bullet}_{HCl}$ crystals (0.0044) also indicates that the hydrogen bond in catalase is not as strong as that of the model system. The catalase *g*-anisotropy is comparable to that of the PSII tyrosyl radicals (0.00535 and 0.00523 for $Tyr^{\bullet}_{PSII-D}$ and $Tyr^{\bullet}_{PSII-Z}$, respectively) as well as for the mouse and herpes RNR (0.0054) (Table 1). Presumably, the observed *g*-anisotropy for the catalase radical, like for PSII, reflects an intermediate hydrogen bond strength.

An interesting feature of the catalase tyrosyl radical is the width and the shape of the g_x edge of the HF-EPR spectrum (Figure 2A). The g_x component of the $Tyr^{\bullet}_{CAT}$ is significantly broader than that of the $Tyr^{\bullet}_{RNR}$. As with the $Tyr^{\bullet}_{PSII-Z}$,[27] this broadness is interpreted as arising from the existence of a distribution in strengths of the hydrogen bonding to the catalase radical.[61] The asymmetric shape of the g_x component of the $Tyr^{\bullet}_{CAT}$ at pH 6.7 is indicative of the presence of a majority of radicals (*g*-anisotropy of 0.00529) with an intermediate hydrogen bond strength and a minority (*g*-anisotropy of 0.00446) with a strong hydrogen bond, comparable to that observed for the $Tyr^{\bullet}_{HCl}$. At low pH, the hydrogen bond strength to the majority of the $Tyr^{\bullet}_{CAT}$ becomes weaker (*g*-anisotropy of 0.00563), and the minor feature exhibits *g* values (*g*-anisotropy of 0.00615) that are comparable to those of the *E. coli* $Tyr^{\bullet}_{RNR}$ (*g*-anisotropy of 0.00666 or 0.00687) and indicative of very weak or no hydrogen bond interactions. The net effect of lowering the pH from 6.7 to 4.5 in the catalase tyrosyl radical appears to be, on the average, the weakening of the hydrogen bond(s).

Vibrational Frequencies of the Catalase Tyrosyl Radical. The vibrational frequencies of *in vitro* phenoxy radical and its derivatives have been thoroughly studied by using RR spectroscopy.[18,47,62] In contrast, the vibrational spectra of only a few protein tyrosyl radicals have been published to date: the tyrosyl radical of *E. coli* RNR,[15] galactose oxidase,[16] and glyoxal oxidase.[17] The tyrosyl radicals in the galactose and glyoxal oxidases are coordinated to the metal active site.[17,63,64] It has been shown by a series of metal-coordinated phenoxy radicals and density functional calculations that the vibrational frequency of the ν_{8a} mode and the energy difference between the ν_{8a} and ν_{7a} modes of phenoxy radicals can be used to discriminate whether the radical is coordinated to a metal center.[23] For noncoordinated radicals, the energy difference between ν_{8a} and ν_{7a} is 50−80 cm^{-1}, and higher than 100 cm^{-1} for the coordinated radicals.[23,65] However, these calculations did not take into account the hydrogen-bonding effect.[23] If one assumes that differences between noncoordinated and metal-coordinated tyrosyl radicals are largely due to electrostatic interactions between the metal and the radical, one would predict hydrogen bonding to represent an intermediate case with an energy range between these extreme values depending on the hydrogen bond strength. The energy difference between the ν_{8a} (1574 cm^{-1}) and the ν_{7a} (1484 cm^{-1}) modes of the catalase tyrosyl radical, 90 cm^{-1}, appears to be in good agreement with such a situation.

For *E. coli* RNR, the band observed at 1498 cm^{-1} in the RR spectrum excited at 406.7 nm was assigned to the ν_{7a} stretching mode of the C−O bond of a noncoordinated and non-hydrogen-bonded tyrosyl radical.[15] Based on classical measurements on alcohols and ketones, the vibrational frequency of the C−O stretching mode is expected to decrease upon hydrogen bond formation.[66] The lower frequency observed for the C−O vibrational mode of the $Tyr^{\bullet}_{CAT}$ (1484 cm^{-1}) as compared to that of $Tyr^{\bullet}_{RNR}$ (1498 cm^{-1}) is consistent with the presence of a hydrogen bond to the radical and in agreement with the HF-EPR results. Moreover, the 4-cm^{-1} upshift observed for the ν_{7a} band of the $Tyr^{\bullet}_{CAT}$ at low pH (1488 cm^{-1}) compared to that at higher pH (1484 cm^{-1}) implies a weakening of the hydrogen bond(s) on the $Tyr^{\bullet}_{CAT}$. This effect is consistent with the observed increase of 0.0002 on the g_x value at acidic pH (see Table 1), due to a weakening of the hydrogen bond. An interesting result is the considerable broadening observed for the ν_{7a} bandwidth in the RR spectrum of $Tyr^{\bullet}_{CAT}$ at acidic pH (9 cm^{-1} at pH = 6.7, 16 cm^{-1} at pH = 4.5), denoting the contribution of hydrogen bonds of different strengths. This effect correlates well with the observed broadening (or the increase in the Gaussian distribution) of the g_x edge of the HF-EPR spectrum (0.00047 at pH = 6.7, 0.00067 at pH = 4.5). It is intriguing that, while the tyrosyl radicals in catalase and PSII are all hydrogen bonded (see above) and thus have similar g_x values, the vibrational bands of the ν_{7a} modes obtained from the FTIR difference spectra[21,22] for $Tyr^{\bullet}_{PSII-D}$ (1503 cm^{-1}) and $Tyr^{\bullet}_{PSII-Z}$ (1512 cm^{-1}) are observed at significantly higher vibrational frequencies than that of the catalase Tyr• (1484/1488 cm^{-1}) and even higher than that reported for the RNR isolated radical (1498 cm^{-1}). To understand these apparently conflicting results, we performed *ab initio* density functional calculations.

Theoretical *g* Values and Vibrational Frequencies (ν_{7a}-(C−O) Stretching Mode) of Tyrosyl Radicals in Different Environments. As shown in Figure 5B, the total energy of the *p*-methylphenoxy−water complex decreased with decreasing $C-O\cdots H_{water}$ distance, indicating the formation of a hydrogen bond. Below a $C-O\cdots H_{water}$ distance of 1.7 Å, the total energy sharply increased, presumably due to Coulombic repulsion.

(59) Frey, M. N.; Koetzle, T. F.; Lehman, M. S.; Hamilton, W. C. *J. Chem. Phys.* **1973**, *58*, 2547−2556.

(60) As shown in Table 1, for comparison of g_x values, it is important to consider the difference $\Delta g = |g_x - g_z|$, since as mentioned before, g_z is invariant, and thus Δg accounts for differences arising from the spectrometers. Thus, the comparable g_x value would be 2.0065.

(61) Multifrequency EPR studies (95, 190, and 285 GHz) show that the broadness of the g_x edge scales with microwave frequency; therefore, we exclude the spin−spin interactions as the origin of this broadness.

(62) Mukherjee, A.; McGlashen, M. L.; Spiro, T. G. *J. Phys. Chem.* **1995**, *99*, 4912−4917.

(63) Babcock, G. T.; El-Deeb, M. K.; Sandusky, P. O.; Whittaker, M. M.; Whittaker, J. W. *J. Am. Chem. Soc.* **1992**, *114*, 3727−3734.

(64) Whittaker, M. M.; Chuang, Y. Y.; Whittaker, J. W. *J. Am. Chem. Soc.* **1993**, *115*, 10029−10035.

(65) Sokolowski, A.; Leutbecher, H.; Weyhermüler, T.; Schnepf, R.; Bothe, E.; Bill, E.; Hildebrandt, P.; Wieghardt, K. *J. Biol. Chem.* **1997**, *2*, 444−453.

(66) Pinmentel, G. C.; McClellan, A. L. *The Hydrogen Bond*; W. H. Freeman: San Francisco, CA, 1960; pp 255−293.

Interestingly, the optimized C−O bond distance exactly mirrored the total energy. The bond distance first decreased with decreasing hydrogen bond distances (Figure 5A). The calculated vibrational frequency of the C−O stretching mode (ν_{7a}) increased with decreasing hydrogen bond distances down to 1.7 Å. However, when the distance is shorter than 1.7 Å, the ν_{7a} frequency rapidly decreases. The calculated behavior of the vibrational frequency of the ν_{7a} mode is clearly qualitatively consistent with the experimental observations on the protein tyrosyl radical if one assumes that $Tyr^{\bullet}_{RNR}$, $Tyr^{\bullet}_{PSII-D}$, and $Tyr^{\bullet}_{CAT}$ represent a trend toward stronger hydrogen bonds. It is difficult to make a quantitative assessment due to the lack of accurate experimental information on the hydrogen bond distances, since no high-resolution PSII crystal structure is yet available and there are ambiguities in the identification of the tyrosine residue being the catalase radical site. Nonetheless, ENDOR spectroscopy has shown that the $Tyr^{\bullet}_{PSII-D}$ is hydrogen bonded.[12] The observed hyperfine couplings indicate a hydrogen bond distance of approximately 1.85 Å.[67,68] The calculated value for the vibrational frequency of the ν_{7a} mode is entirely consistent with the observed frequency (Table 2) and the EPR-derived distance. One of the putative hydrogen donors, His 189, has been mutated to a glutamine residue in *Synechocystis* PSII.[12,67] For this PSII mutant, the observed frequency of the ν_{7a} mode in the FTIR difference spectrum was 1497 cm^{-1},[22] the same frequency as that observed in the *E. coli* RNR resonance Raman spectrum.[15]

The calculated values are in good agreement with the corresponding experimental values obtained from proteins (Table 2). However, the maximum value for the ν_{7a} mode appears to be underestimated when compared to values obtained for photochemically generated phenoxy and *p*-methylphenoxy radicals in basic aqueous solution. Several studies obtained the values of 1517 cm^{-1} for the *p*-methylphenoxy radical[50] and 1505 cm^{-1} for the phenoxy radical.[18,47,50,62] These values are about 14 and 6 cm^{-1} higher than those predicted by our calculations for the phenoxy and *p*-methylphenoxy radicals, respectively. The latter value is well within the error range observed for the other modes (see Table 2), and the former is larger than expected. The discrepancy between calculated and experimental values is unlikely to be due to the number of hydrogen bonds, as shown by Figure 6. The maximum vibrational frequency of the ν_{7a} mode of the phenoxy radical is essentially the same whether the radical is hydrogen bonded to one or two water molecules, the only difference being the hydrogen bond distance at which the maximum occurs (Figure 6, top). However, it is likely that the local environment of the tyrosyl radical in reality is more complicated than the simple radical−water complex considered here. For example, the electrostatic effect of cations in solution needs to be considered.[69] Another possibility is that the calculations significantly underestimate the ν_{7a} frequency in this distance, and even more dramatic behavior occurs. Whether the difference between the calculated and the experimental values reflects an underestimation by the calculations or real differences, it is clear that the observed shift toward high vibrational frequencies due to the presence of a hydrogen bond at distances longer than 1.7 Å is accurately reproduced by the density functional calculations. A possible origin of this unusual hydrogen-bonding effect lies in the fact that the unpaired electron of the tyrosyl radical resides in an antibonding orbital. The density functional calculations show that the net charge on the oxygen, as determined from Mulliken population analysis, remains approximately constant with changes in hydrogen-bonding distances, indicating that the electrons polarized toward the oxygen atoms, via the σ-bonds, are offset by reduction in charge via the π-bonds. This reduces the antibonding character, leading to a stronger C−O bond. Calculations also show that an optimal hydrogen bond reduces the energy of the antibonding orbital by 5%, further indicating reduction in antibonding character.

Another important prediction of our calculations is a very sharp decrease in vibrational frequencies for relatively short hydrogen-bonding distance (shorter than 1.7 Å). For the one-water−*p*-methylphenoxy radical complex, the frequency of the ν_{7a} mode decreases from 1503 cm^{-1} for a hydrogen bond distance of 1.7 Å to 1490 cm^{-1} for a distance of 1.5 Å. A similar decrease in frequency is observed for the one-water−phenoxy radical complex. The steepness of the downshift with respect to hydrogen-bonding distances strongly suggests the possibility of inhomogeneous broadening of the ν_{7a} mode due to a small disorder in the electrostatic microenvironment of the radical. Assuming that the simple radical−water(s) complex is a sufficient model for the radical behavior in solution and in the protein, then it seems unlikely that such a condition would arise in solution, as the frequency maximum corresponds to maximum hydrogen bond strength. However, within a more constrained environment, like that of the protein, such an inhomogeneous broadening may be observable. The experimental vibrational frequency of the ν_{7a} mode observed for the catalase tyrosyl radical is 1484 cm^{-1} at high pH values. A frequency upshift of 4 cm^{-1} and a line broadening of 7 cm^{-1} were observed when the pH was lowered to 4.5. Based on *p*-methylphenoxy radical calculations, the 1484-cm^{-1} vibrational frequency corresponds to a distance of approximately 1.45 Å (Figure 6, top). If a second hydrogen bond to the radical is present, a distance of 1.60 Å would be predicted.[70] Assuming the presence of two hydrogen bonds to the *p*-methylphenoxy radical, a distance elongation of 0.07 Å (from 1.60 to 1.67 Å) results in an upshift of 12 cm^{-1} of the ν_{7a} vibrational frequency (see Figure 6, top). Consequently, the behavior predicted by the calculations is consistent with the experimental results if one assumes a small elongation in the hydrogen bond for distances about 1.6 Å, but lower than 1.7 Å. From the crystal structure data,[71,72] Tyr 259 and Tyr 369 have an aspartate residue at hydrogen bond distances of 1.45 and 1.58 Å, respectively, together with a structural water molecule. Both tyrosine residues are considered good candidates for the radical site (see below).

Finally, we address the relationship of the vibrational frequency of the ν_{7a} mode and the g_x values of tyrosyl radicals. As Figure 6 suggests, this relationship is not expected to be simple. The g_x values monotonically decrease with decreasing hydrogen bond distance, while the vibrational frequency of the ν_{7a} mode increases slightly and then decreases sharply. While for weak to modest hydrogen bonds (2.0 to 1.7 Å) the g_x values are predicted to be more sensitive to strengthening of the

(67) Tang, X.-S.; Zheng, M.; Chisholm, D. A.; Dismukes, C. G.; Diner, B. A. *Biochemistry* **1996**, *35*, 1475−1484.

(68) Diner, B. A.; Force, D. A.; Randall, D. W.; Britt, R. D. *Biochemistry* **1998**, *37*, 17931−17943.

(69) The radicals were generated in buffer solutions containing NaOH.

(70) A direct addition of 14 cm^{-1} to the calculated (ν_{7a}) vibrational frequency for the phenoxy radical complexed with two water molecules (Table 2) would give the expected vibrational frequency for the ν_{7a} mode of a *p*-methylphenoxy radical complexed with two water molecules.

(71) Murthy, M. R. N.; Reid, T. J.; Sicignano, A.; Tanaka, N.; Rossman, M. G. *J. Mol. Biol.* **1981**, *152*, 465−499.

(72) (a) Fita, I.; Rossman, M. G. *J. Mol. Biol.* **1985**, *185*, 21−37. (b) Fita, I.; Silva, A. M.; Murthy, M. R. N.; Rossman, M. G. *Acta Crystallogr.* **1986**, *B42*, 497−515.

(73) Dollish, F. R.; Fateley, W. G.; Bentley, F. F. *Characteristic Raman Frequencies of Organic Compounds*; Wiley: New York, 1974.

hydrogen bond, the opposite is true for stronger hydrogen bonds. Apparently, g_x values and ν_{7a} frequencies are not strictly correlated. When disorder in hydrogen bonding is considered, the comparison becomes complex and strongly depends on the nature of the hydrogen bond. Unlike g_x values, the ν_{7a} vibrational frequency dependence on hydrogen bonding is complex, and a symmetric distribution in hydrogen bond distances will not, in general, lead to symmetrical line shapes. This behavior provides a partial explanation for the apparent disparity between the FTIR and HF-EPR results on the $Tyr^{\bullet}_{PSII-Z}$. For the $Tyr^{\bullet}_{PSII-D}$ and $Tyr^{\bullet}_{RNR}$, the line width of the ν_{7a} mode is about 9 cm^{-1}. For $Tyr^{\bullet}_{PSII-Z}$, the line width was found to be 13 cm^{-1}, with a maximum at 1512 cm^{-1}, as compared to 1503 cm^{-1} for $Tyr^{\bullet}_{PSII-D}$. For hydrogen bond distances higher than 1.7 Å, the modest increase of 4 cm^{-1} in the line width can correspond to a large range of distances (see Figure 6, top). The difference in the quoted C−O frequencies, which were measured at peak maxima of the differential band, could be due, in part, to the asymmetric line shape, for which the maximum does not correspond to the average. If the hydrogen bond effect on the ν_{7a} mode is much larger than that predicted by the calculations, as indicated by the experimental data, the problem originating from highly asymmetric line shapes will be also greater. However, it is clear that there is little discrepancy between the FTIR and HF-EPR measurements on the PSII tyrosyl radicals.

As mentioned before, our density function calculations (Figure 6, top) predict a distance of about 1.6 Å for the experimental vibrational frequency (1484 cm^{-1}) of the $Tyr^{\bullet}_{CAT}$ ν_{7a} mode. The calculated g_x values for the two-water−*p*-methylphenoxy radical complex corresponding to a hydrogen bond distance of 1.6 Å appears to be slightly lower than the experimental value obtained at high pH. However, in light of the observed distribution in g_x values, the agreement is quite good. The distribution in g_x values for the $Tyr^{\bullet}_{CAT}$ (pH 6.9), from 2.0074 to 2.0065, implies calculated hydrogen-bonding distances between 1.6 and 1.7 Å (Figure 6, bottom). At low pH, the observed distribution in g values is larger, and the agreement with the calculated values is less satisfying. Both the HF-EPR and resonance Raman results on the $Tyr^{\bullet}_{CAT}$ argue for the presence of at least one hydrogen bond to the radical. The pH dependence of the HF-EPR spectra is mostly consistent with the presence of two species interacting with the radical, one of which having a p*K* close to 4.5. Under these considerations, the inspection of the local environment of all tyrosine residues in the catalase crystal structure[71,72] allowed us to propose Tyr 259 and Tyr 369 as good candidates for the radical site. Both of these tyrosine residues have an aspartate residue and a structural water molecule nearby. Specifically, Tyr 259 has an Asp at an $O_{Asp}\cdots O_{Tyr}$ distance of 2.45 Å (actual hydrogen bond distance of 1.45 Å) and a water molecule at an $O_w\cdots O_{Tyr}$ distance of 6 Å. For Tyr 369, the phenolic oxygen is 2.58 Å away from the closer oxygen of Asp 334 (thus the actual hydrogen bond distance is 1.58 Å) and a water molecule at an $O_w\cdots O_{Tyr}$ distance of 4.3 Å. In addition, the proximal nitrogen (N_ϵ) of His 361 is 4.0 Å away from the Tyr 369 phenolic oxygen. From the structural data, His 361 appears to be too far away to form a hydrogen bond. Nevertheless, a minor repositioning would result in a reasonable distance for hydrogen bond formation to the radical or, alternatively, to the aspartate. Although we have not been able to shed light on the site of the catalase tyrosyl radical, the spectroscopic response of this radical to pH variations has greatly clarified the relationship between the vibrational frequency of the ν_{7a} mode, the g_x values, and the microenvironmental effects such as hydrogen bonding. These results point to the utility of combining vibrational spectroscopy and high-field EPR to the study of radicals in proteins.

Acknowledgment. We thank A. William Rutherford for his support of this work and for critically reading the manuscript. We also thank Alain Boussac, Alain Desbois, Pierre Dorlet, and Jonathan Hanley for stimulating discussions. This work was supported through the European Union HCM-Research Network (contract no. FMRX-CT98-0214) and the Human Frontiers Science Organization (contract no. RGO349).

JA990562M